# Synthetic and Predictive Approach to Unsymmetrical Biphenols by Iron-Catalyzed Chelated Radical–Anion Oxidative Coupling

Anna Libman,[†] Hadas Shalit,[†] Yulia Vainer, Sachin Narute, Sebastian Kozuch, and Doron Pappo*

Department of Chemistry, Ben-Gurion University of the Negev, Beer-Sheva 84105, Israel

S *Supporting Information*

ABSTRACT: An iron-catalyzed oxidative unsymmetrical biphenol coupling in 1,1,1,3,3,3-hexafluoropropan-2-ol that proceeds via a chelated radical–anion coupling mechanism was developed. Based on mechanistic studies, electrochemical methods, and density functional theory calculations, we suggest a general model that enables prediction of the feasibility of cross-coupling for a given pair of phenols.
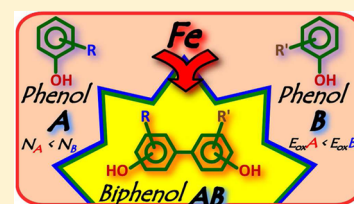
INTRODUCTION

Metal-catalyzed oxidative coupling of phenols offers a direct approach to the synthesis of complex phenol-based materials in an atom- and step-economic fashion. Such compounds are widely used in many applications, including catalysis[1] and synthesis of natural products, pharmaceutical compounds, and polymers.[2] Over the years, the chemo- and regioselective syntheses of biphenols, with control over the coupling mode (C–C vs C–O) and the coupling sites (*ortho-ortho*, *ortho-para*, or *para-para*), have become well-established chemistry. A less common—but more intriguing and highly important—transformation is the oxidative cross-coupling reaction between two phenol coupling partners with similar chemical and physical properties to produce unsymmetrical biphenols.[1a,3] In an early work, Hovorka and Zavada[3n−p] introduced a stoichiometric Cu(II)/amine-mediated system to cross-couple substituted 2-naphthols.[3k] Later, Katsuki's

group described an aerobic enantioselective cross-coupling of 2-naphthols by an iron(salan) complex that relies on selective coupling between an iron-bound 3-substituted naphthoxyl radical (phenolic component **A**) and an uncoordinated nucleophilic 6-substituted 2-naphthol partner (phenolic component **B**).[3e] A similar mechanism was proposed by the group of Kozlowski for the Cr-salen-catalyzed cross-coupling of 2,6-dialkylphenols with various phenols.[3b] An alternative, metal-free route to unsymmetrical biphenols by an anodic oxidative cross-coupling method was subsequently developed by Waldvogel and colleagues.[3c]

Despite the considerable work that has been conducted on these reactions, only limited attempts have been made to explain the observed chemoselectivity in the oxidative cross-coupling of
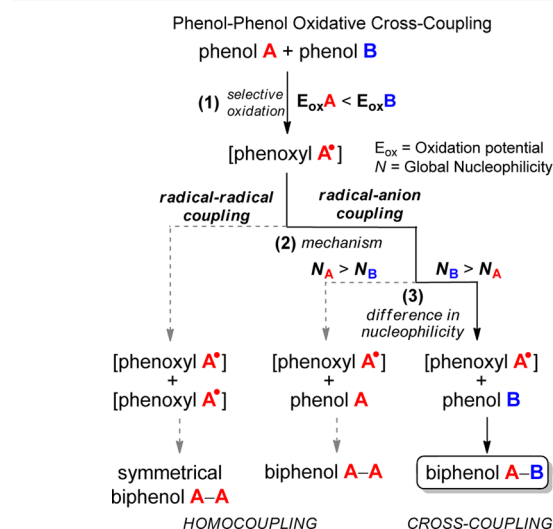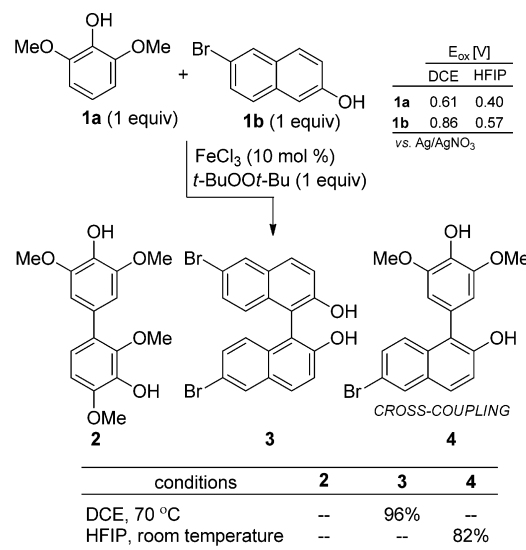
Figure 1. General principles for the cross-coupling of phenols: (1) selective oxidation of phenol **A**; (2) radical–anion mechanism; and (3) higher nucleophilicity of phenol **B**.

Scheme 1. Oxidative Coupling of 2,6-Dimethoxyphenol (1a) and 6-Bromo-2-naphthol (1b)

E_ox [V]		
	DCE	HFIP
1a	0.61	0.40
1b	0.86	0.57
vs. Ag/AgNO_3		

conditions	2	3	4
DCE, 70 °C	--	96%	--
HFIP, room temperature	--	--	82%

phenols. Hovorka and Zavada suggested that a binuclear Cu(II) complex comprising metal centers with different redox potentials accounts for the chemoselectivity in the intramolecular oxidative naphthol/naphthol and naphthol/naphthylamine coupling by their Cu(II)/amine system.[3o] Later, based on electrochemical measurements and frontier molecular orbital theory, Kočovský et al. postulated that the reaction involves the coupling between an electrophilic radical and an anionic acceptor,[3k] and that cross-coupling is preferred when there is a sufficient difference in the redox potentials ($\Delta E \geq 0.25$ V) of the two coupling partners.[1a] Nevertheless, a general approach to elucidate the elements of selectivity in phenol−phenol oxidative coupling reactions and that could serve as a prediction tool is still lacking.
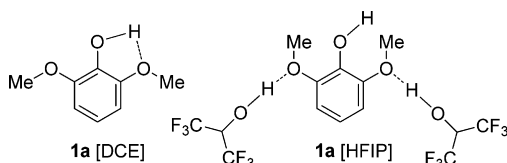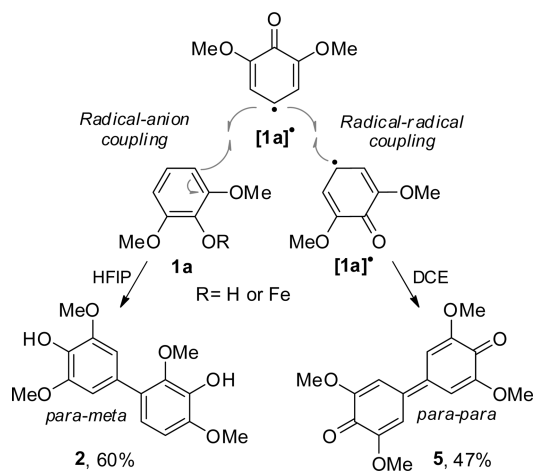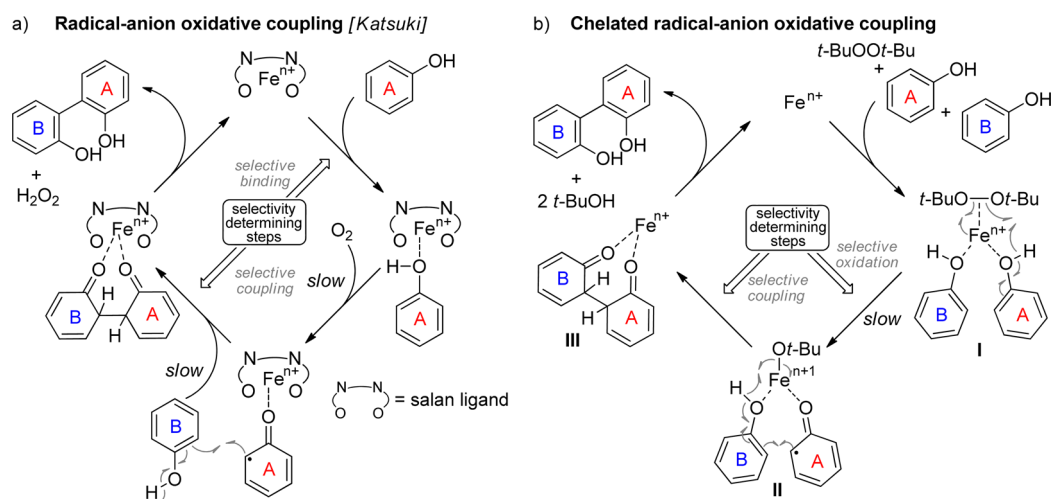

Figure 2. Proposed structure of phenol **1a** in different solvents.

Scheme 2. Oxidation of 1a under Radical−Radical (*para-para*) and Radical−Anion (*para-meta*) Coupling Mechanisms

In parallel to the development of the above-described reactions, our group's ongoing research program[4] has focused on the iron-catalyzed cross-dehydrogenative coupling (CDC)[5] of phenols,[6] and within this framework, we examined an oxidative biphenol coupling reaction using a simple FeCl$_3$ salt as the catalyst. Intrigued by the mechanistic questions raised by the phenol−phenol oxidative coupling, we aimed to develop a rational and predictable approach toward the synthesis of unsymmetrical biphenols. For this purpose, similar to Kočovský,[3k] we hypothesized and tested the premise that oxidative cross-coupling would be favorable if

(1) phenol **A** undergoes selective oxidation to a phenoxyl **A•** radical in the presence of phenol **B** ($E_{ox}\mathbf{A} < E_{ox}\mathbf{B}$, Figure 1 (1))
(2) the coupling takes place via a radical−anion coupling mechanism[5i,j] (Figure 1 (2))
(3) phenol **B** is a stronger nucleophile than phenol **A** ($N_{\mathbf{B}} > N_{\mathbf{A}}$, where N is the theoretical global nucleophilicity; Figure 1 (3)).

In this study, an efficient phenol−phenol oxidative cross-coupling reaction was developed using a sustainable iron catalyst. Based on kinetic studies, a chelated radical−anion coupling mechanism was postulated. With the aim of identifying types **A** and **B** phenolic components that are compatible for cross-coupling, the oxidation potentials and the theoretical global nucleophilicity values of a large number of phenols were determined, and a predictive model for the preparation of unsymmetrical biphenols was proposed and examined.

■ RESULTS AND DISCUSSION

Method Development and Mechanistic Study. The research was initiated by studying the phenol−phenol CDC reaction between 2,6-dimethoxyphenol (**1a**, 1 equiv) and 6-bromo-2-naphthol (**1b**, 1 equiv, Scheme 1). When the reaction was performed in 1,2-dichloroethane (DCE, 0.5 M) at 70 °C, with FeCl$_3$ (10 mol %) as the catalyst and *t*-BuOO*t*-Bu (1 equiv) as the terminal oxidant, homodimerization of 6-bromo-2-naphthol **1b** occurred, affording BINOL **3** in 96% yield. To obtain cross-coupling rather than homodimerization, we exploited our group's recent findings that 1,1,1,3,3,3-hexafluoropropan-2-ol (HFIP)[7] has a significant effect on the efficiency and selectivity of

Scheme 3. Proposed Iron(Salan)-Catalyzed Radical−Anion Oxidative Coupling (a) and Metal-Catalyzed Chelated Radical−Anion Coupling (b) Mechanisms

iron-catalyzed oxidative cross-coupling reactions between phenols and various nucleophilies.[4a] It has been suggested that fluoroalcohols stabilize electrophilic radical species,[8] which become persistent and react with the appropriate nucleophiles.[8a,c] Indeed, when the above coupling reaction was performed in HFIP (instead of DCE) at room temperature, a cross-coupling reaction took place, producing unsymmetrical biphenol **4** as a single product in 82% yield (Scheme 1). The fact that only **1b** underwent oxidation in DCE, even though it has a higher oxidation potential than **1a** (Scheme 1, inserted table), emphasizes the importance of phenol−metal binding during the oxidation step. We, therefore, suggest that, in the aprotic DCE solvent, the −OH group of **1a** forms an intramolecular hydrogen bond with the "remote" *ortho*-OMe substituents (Figure 2, structure **1a** [DCE])[9] and thus exhibits reduced availability for metal binding. As a result, the oxidation of the chelated naphthol **1b** is preferable. In contrast, in HFIP, the *ortho*-OMe groups of **1a** are bound to the hydrogen-bond-donating solvent (structure **1a** [HFIP]);[8d,10] the "liberated" −OH group binds to the iron catalyst and, since it has lower oxidation potential than **1b**, undergoes selective oxidation.

The mechanistic distinction between the oxidative coupling reactions in the different solvents was further emphasized when **1a** was subjected to homocoupling reactions (cat. FeCl₃, *t*-BuOO*t*-Bu). The reaction in DCE at 70 °C resulted in the symmetrical product diphenoquinone **5** in 47% yield (Scheme 2), while unsymmetrical biphenol **2** was obtained as a single product in 60% yield when the reaction was performed in HFIP. Several types of oxidative cross-coupling mechanisms for phenols that involve radical−radical[2,3g] and radical−anion coupling have been proposed.[3e,f,k,p] The formation of **5** is known to proceed via an outer-sphere homolytic coupling of two free *para*-phenoxyl radicals (Scheme 2),[2,3o,11] while the formation of **2** likely involves the coupling of the chelated *para*-phenoxyl radical with the most nucleophilic *meta*-position of the ground-state phenol **1a**. The homocoupling of 2,6-dimethoxyphenol (**1a**) can thus serve as a mechanistic probe to distinguish between radical−radical and radical−anion coupling modes.[11c]

Kinetic Studies. To further probe the mechanism of the iron-catalyzed oxidative biphenol coupling reaction in HFIP, we performed kinetic studies of the homocoupling of 2,6-dimethoxyphenol (**1a**) and 2-naphthol (**1c**; see Supporting Information) in HFIP, as was done by Katsuki et al. for the aerobic oxidative homocoupling of **1c** by an iron(salan) complex (Scheme 3a). Their results showed a first-order dependence on the oxygen molecule and on the coupling substrate; therefore, a coupling between a chelated phenoxyl A• radical and an un-coordinated nucleophilic phenol **B** was suggested (Scheme 3a).[3e] In contrast, our initial kinetic experiments revealed that, under CDC conditions, the reaction rate depends solely on the concentration of the multicoordinated iron catalyst (Figure 3A), with zero-order dependence on the oxidant (*t*-BuOO*t*-Bu, Figure 3B) and the coupling substrate (Figure 3C). Thus, on the basis of the kinetic studies and the results given above, we propose the chelated radical−anion coupling mechanism shown in Scheme 3b.[3b,e,g] The first step of the mechanism is the reversible binding of the phenolic components **A** and **B** and the peroxide to the iron salt (complex **I**). Peroxide bond cleavage by the metal, which is likely the rate-determining step,[3e] followed by a single electron transformation (SET) process, forms a bound phenoxyl A• radical (complex **II**). The latter electrophile reacts with the chelated phenol(ate) **B** (complex **III**) or with a second chelated phenol(ate) **A** in a homocoupling process. The catalytic cycle is terminated by a ligand-exchange process that liberates
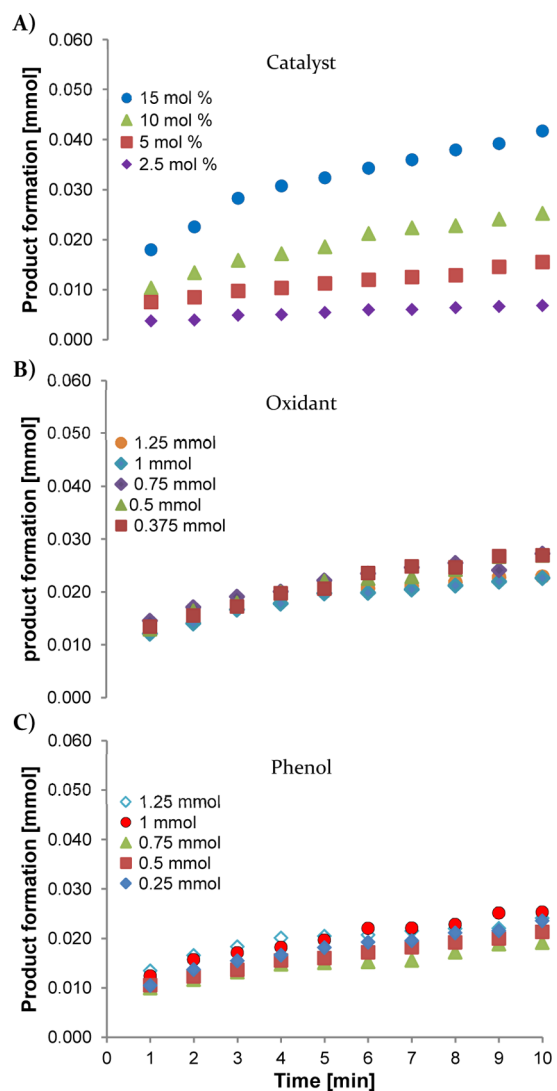

Figure 3. Kinetic study of the iron-catalyzed CDC of 2,6-dimethoxyphenol. General conditions: phenol **1a** (0.25 mmol), FeCl₃ (10 mol %), *t*-BuOO*t*-Bu (0.375 mmol), HFIP (1 mL, 0.25M), 0 °C. (A) Effect of FeCl₃ catalyst concentration on homocoupling formation product of **2**. (B) Effect of *t*-BuOO*t*-Bu concentration on homocoupling formation product of **2**. (C) Effect of substrate **1a** concentration on homocoupling formation product.

both the biphenol and *tert*-butyl alcohol. In this scenario, the phenol oxidation step and the coupling step determine the chemoselectivity of the reaction (Scheme 3b), while the selectivity-determining steps of the structurally defined iron-(salan) complex that the Katsuki group found were the selective binding of phenol **A** to the complex and the intermolecular coupling (Scheme 3a). The discovery that the two catalytic systems differ in their mechanistic schemes is particularly important for the future development of improved catalytic systems with good control over the chemo- and stereoselectivity.

Predictive Model. Next, we sought to identify the factors that control the chemoselectivity in phenol−phenol oxidative cross-coupling reactions. Previous reports demonstrated that the oxidation potential of phenols depends on the O−H bond dissociation energy (BDE), which is controlled by the local electronic properties of the phenol group.[9b,12] In contrast, the nucleophilicity is related to the energy of the highest occupied molecular orbital (HOMO), which is a global molecular property.[13]

Table 1. Oxidation Potentials in HFIP and Calculated Global Nucleophilicity N Values of 2-Naphthol Derivatives (entries 1−7) and Various Phenols (entries 8−40)

#	phenol	N (eV)[a]	E_{ox} (V)[b]	#	phenol	N (eV)[a]	E_{ox} (V)[b]
1	6-methoxy-2-naphthol	3.95[c]	0.44	21	2-methoxyphenol (**1e**)	3.59	0.51
2	1-methyl-2-naphthol	3.67[c]	0.48	22	3,5-dimethoxyphenol (**1r**)	3.51	0.69
3	2-naphthol (**1c**)	3.57[c]	0.48	23	2,4-dihydroxytoluene	3.48	0.55
4	3-carbomethoxy-2-naphthol	3.46[c]	0.80	24	2,4-dimethylphenol (**1d**)	3.46	0.47
5	6-bromo-2-naphthol (**1b**)	3.40[c]	0.57	25	3,4-dimethylphenol	3.43	0.55
6	3-bromo-2-naphthol (**1p**)	3.27[c]	0.71	26	2,6-di-*tert*-butylphenol (**1n**)	3.43	0.92
7	6-carbomethoxy-2-naphthol (**1o**)	3.24[c]	0.66	27	3-methoxyphenol	3.40	0.60
8	3,4,5-trimethoxyphenol (**1l**)	4.27	0.46	28	2,6-dimethylphenol	3.35	0.54
9	2,5-dimethoxyphenol	4.00	0.48	29	4-*tert*-butylphenol (**1i**)	3.32	0.60
10	3,4-dimethoxyphenol	3.97	0.42	30	4-methylphenol (**1h**)	3.32	0.56
11	2,4-dimethoxyphenol (**1k**)	3.95	0.34	31	2,3-dimethylphenol	3.32	0.58
12	2-methyl-3,4-dimethoxyphenol	3.81	0.48	32	3,5-dimethylphenol (**1m**)	3.29	0.62
13	2,6-dimethoxyphenol (**1a**)	3.78	0.40	33	2-methylphenol	3.24	0.59
14	2-*tert*-butyl-4-methoxyphenol	3.78	0.42	34	2-*tert*-butylphenol	3.21	0.54
15	3,5-dimethoxy-4-methylphenol	3.76	0.48	35	3-methylphenol	3.18	0.58
16	2-methoxy-5-methylphenol	3.73	0.50	36	phenol	3.08	0.63
17	2-methoxy-4-methylphenol (**1q**)	3.73	0.43	37	4-bromophenol (**1g**)	3.05	0.67
18	2,3,4-trimethoxyphenol	3.73	0.48	38	4-chlorophenol	3.02	0.69
19	4-methoxyphenol (**1f**)	3.70	0.50	39	3-bromophenol	2.80	0.75
20	2-methoxy-6-methylphenol (**1j**)	3.59	0.53	40	3-chlorophenol	2.78	0.76

[a]The N index was calculated by the DFT method at the B3LYP 6-311+G(d,p) level of theory. The energy of the HOMO was referenced against the HOMO energy of TCE according to eq 1. [b]The oxidation potential was determined by means of cyclic voltammetry for the selected phenol (3 mM) with tetrabutylammonium hexafluorophosphate as the supporting electrolyte (50 mM) in HFIP (3 mL) vs Ag/0.01 M AgNO₃ in 0.1 M TBAP/CH₃CN, 50 mV s⁻¹. [c]The true nucleophilic behavior of 2-naphthols is much stronger in practice than the given predicted N values.

Therefore, in a radical−anion coupling that is carried out under acid-catalyzed conditions, the phenoxyl **A•** radical will react with the HOMO of a phenolic partner, **A** or **B**.[3k] Recently, the groups of Domingo[14] and of Roy[15] showed a correlation between the energy of the HOMO of a molecule and its relative nucleophilicity and introduced a global scale of calculated nucleophilicity, N, that can be easily determined by density functional theory (DFT) methods, according to

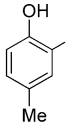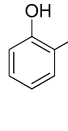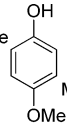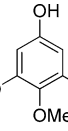$$N_{(phenol)} = E_{HOMO(phenol)} \, (eV) - E_{HOMO(TCE)} \, (eV) \quad \text{(eq 1)}$$

where the energy (E) of the HOMO of tetracyanoethylene (TCE)[14b,15] is used as the reference energy. To evaluate the relative nucleophilicity of a series of phenolic coupling partners, we computed their N values at the B3LYP/6-311+G (d,p) level of theory (see Supporting Information).[14b,15,16] In contrast to many studies that have used the N index to rationalize the relative reactivity of nucleophiles with electrophilic coupling partners,[14a,17] in our work, it was applied to predict the relative reactivity of two nucleophiles with similar properties under competitive oxidation conditions. Therefore, the ΔN value (equal to $N_B − N_A$) for the two phenolic coupling partners was examined.

The N values for the substituted phenols ranged from 1.70 eV for 4-nitrophenol[15] to $N > 4.00$ eV for strong nucleophiles, such as 3,4,5-trimethoxyphenol (**1l**, 4.27 eV). However, despite the utility of the method for evaluating the relative reactivity of nucleophiles, it suffers from several limitations: (1) the DFT calculations do not take into account solvent and metal binding effects that may change the relative nucleophilicity of the phenolic components, and (2) the theoretical N values for the 2-naphthol series failed to predict their true nucleophilicity, which is much stronger in practice than the predicted behavior. Similar discrepancies between the theoretical and the experimental Mayr N index[16] have also been reported for indole derivatives.[14b,15] While the N index can be applied to identify the

phenolic components of type **B**, the phenolic coupling partners of type **A** can be recognized by examining their oxidation potentials. Therefore, we measured, by cyclic voltammetry, the E_{ox} values of a long list of phenols in HFIP, which are listed in Table 1 along with their computed N values.

The data that were collected revealed that the important E_{ox} and N properties do not always agree with each other because they are affected by the type, number, and position of the substituent(s) relative to the −OH group. For example, the measured oxidation potentials of 2,4-dimethylphenol (**1d**, E_{ox} = 0.47 V), 2-methoxyphenol (**1e**, 0.51 V), 4-methoxyphenol (**1f**, 0.50 V), and 3,4,5-trimethoxyphenol (**1l**, 0.46 V) are all in the same range (Table 2), while their calculated nucleophilic power

Table 2. E_{ox} and N Values of Selected Phenols

	1d		**1e**		**1f**		**1l**
E_{ox} [V]	0.47	≈	0.51	≈	0.50	≈	0.46
N [eV]	3.46	<	3.59	<	3.70	<<	4.27

varies from moderate, as in phenol **1d** (N = 3.46 eV), to strong, as in **1l** (4.27 eV). In the current study, we found that the particular utility of the E_{ox} and N properties lies in their combined use to identify the phenolic pairs **A** and **B**, which are characterized by $E_{ox}\mathbf{A} < E_{ox}\mathbf{B}$ and $N_B > N_A$ (i.e., $\Delta N > 0$), and that should be suitable for cross-coupling (see Figure 1); pairs of phenols of this type are thus designated here as "complementary". Such a complementary relationship was observed for 2,6-dimethoxyphenol (**1a**, type **A**) and 6-bromo-2-napthol (**1b**, type **B**), and this complementarity thus explains the high

chemoselectivity obtained when the two phenolic components were reacted in HFIP (Scheme 1).

Our next experiment was designed to further examine the role of the nucleophilicity of the phenolic coupling partners in oxidative cross-coupling reactions. For that purpose, phenol **1a**
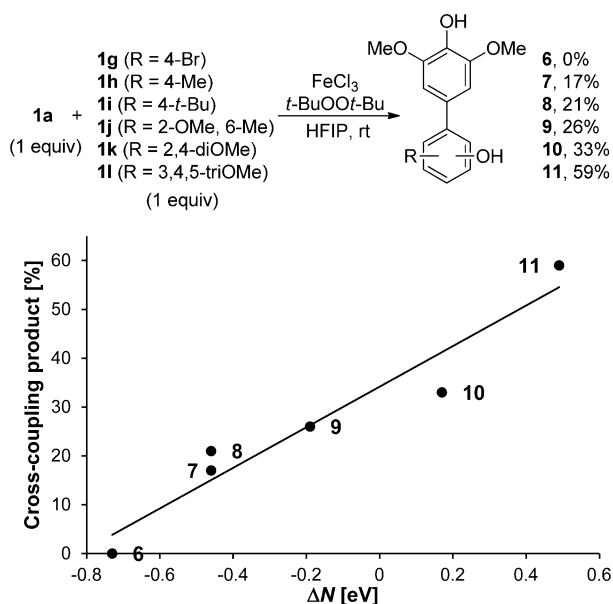
1g (R = 4-Br)
1h (R = 4-Me)
1i (R = 4-*t*-Bu)
1j (R = 2-OMe, 6-Me)
1k (R = 2,4-diOMe)
1l (R = 3,4,5-triOMe)

1a + (1 equiv)
(1 equiv)

$\xrightarrow[\text{HFIP, rt}]{\text{FeCl}_3 \quad t\text{-BuOO}t\text{-Bu}}$

6, 0%
7, 17%
8, 21%
9, 26%
10, 33%
11, 59%

Figure 4. Relation between the ΔN and the cross-coupling efficiency.

Scheme 4. Validation of the E_{ox} and N Values for Other Oxidation Systems

a) Kozlowski:

1m (1 equiv) + **1n** (2 equiv) $\xrightarrow[\text{O}_2, \text{DCE}]{N_B > N_A \quad \text{Cr(Salen) cat.}}$ **12** 56% (91% brsm)

b) Katsuki:

1o (2 equiv) + **1p** (1 equiv) $\xrightarrow[\text{O}_2, \text{PhMe}]{N_B \approx N_A \quad \text{Fe(Salan) cat.}}$ **13** 54%, 93% ee

1p was added in three batches over 24 h.

c) Waldvogel:

1q (1 equiv) + **1d** (3 equiv) $\xrightarrow[\text{HFIP}]{N_B < N_A \quad \text{BDD anode}}$ **14** 52%
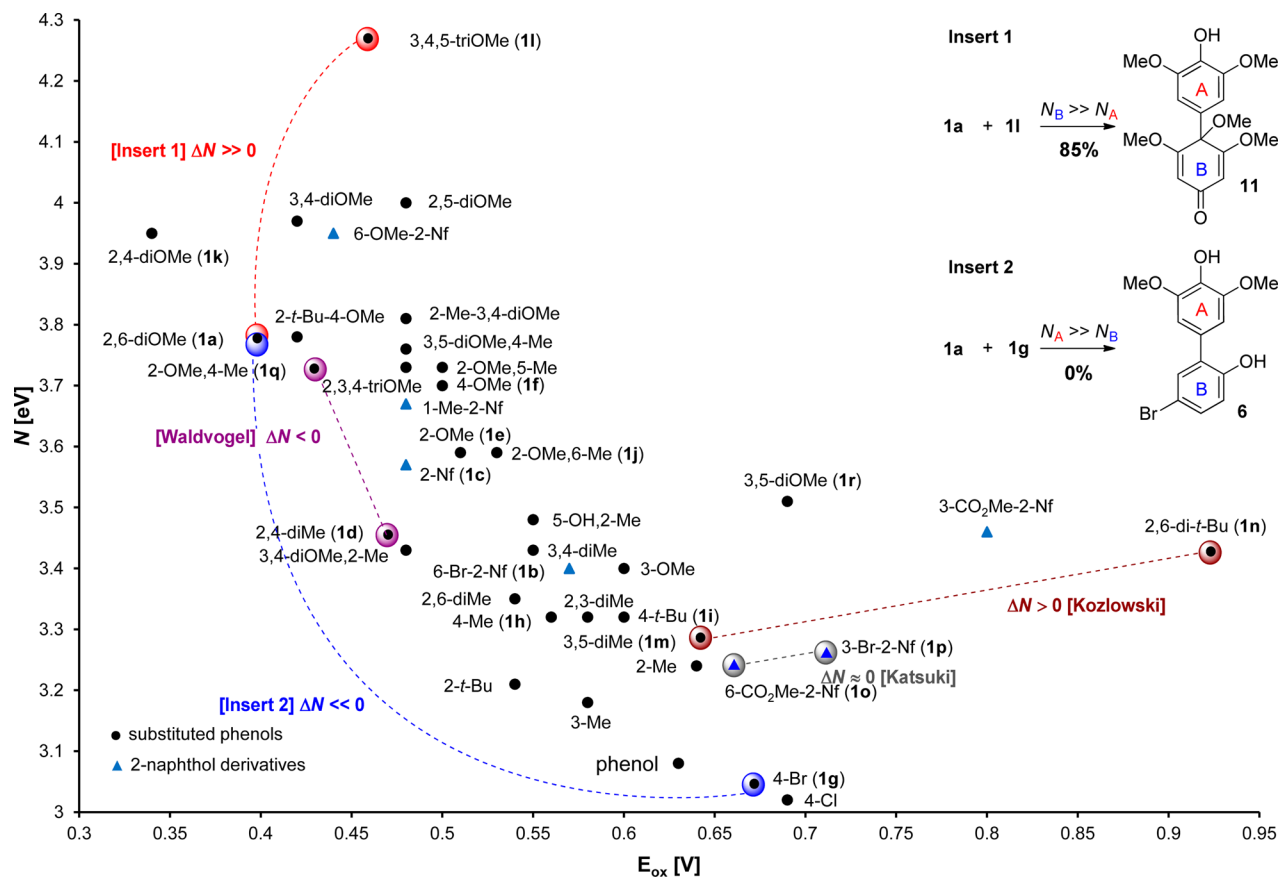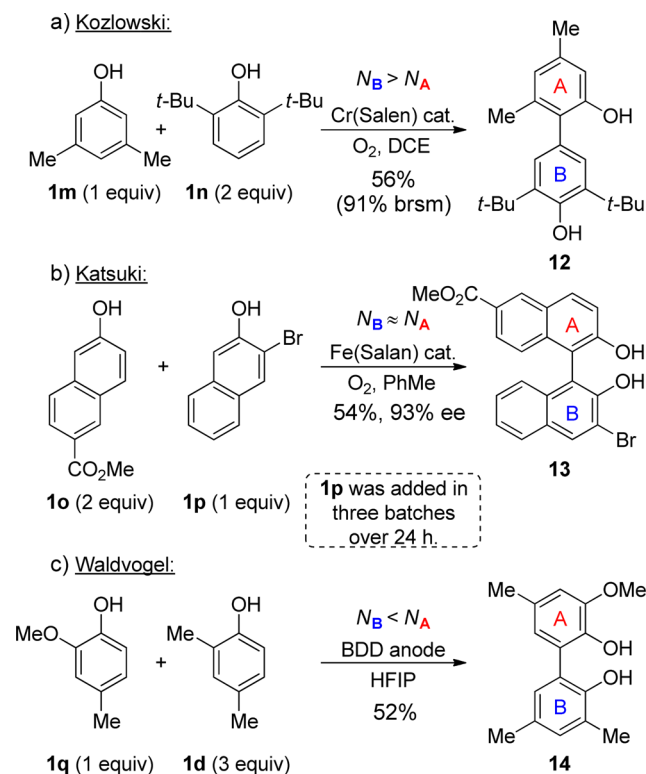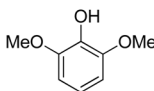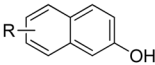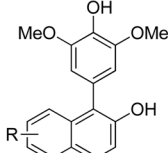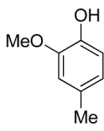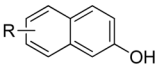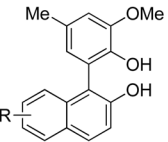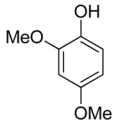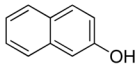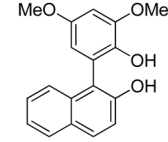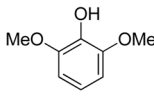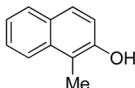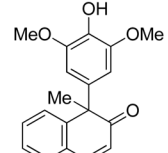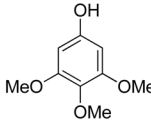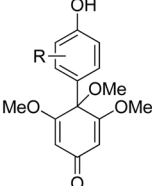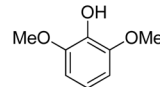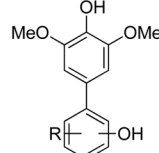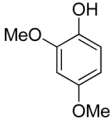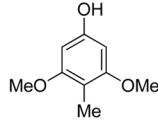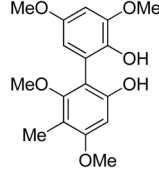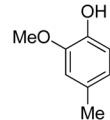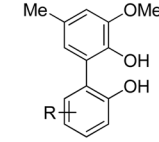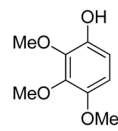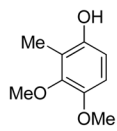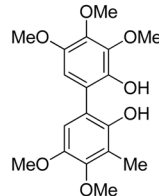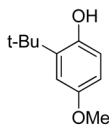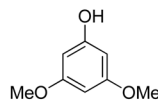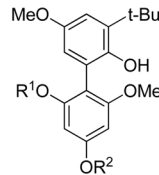
Figure 5. Reactivity map for phenols based on their E_{ox} and N values. The graph enables the identification of phenolic pairs with a complementary relationship. As an example, the red dashed line links phenols **1a** and **1l** that produced a cross-coupling product **11** in high selectivity (insert 1), and thus complementary, while the blue dashed line connects phenols **1a** and **1g** that afforded only the homocoupling product **2** (insert 2).

Table 3. Scope and Yields of Oxidative Unsymmetrical Biphenol Coupling Reactions by an Iron Salt for Systems with $N_B \gg N_A$ and $N_B \approx N_A$

entry	phenol A	phenol B	biphenol A-B
		$N_B \gg N_A$	
1		R = 6-Br	**4**, 96%
2		R = 6-CO$_2$Me	**15**, 95%
3		R = 3-Br	**16**, 87%
4		R = 3-CO$_2$Me	**17**, 54%
5		R = H	**18**, 86%
6		R = 6-Br	**19**, 89%
7		R = 3-Br	**20**, 42%
8		R = 3-CO$_2$Me	**21**, 82%
9			**22**, 47%
10			**23**, 83%
11		R = 2-Me,5-OH	**24**, 71%
12		R = 2,6-diOMe	**11**, 85%
13		R = 2-OMe,6-Me	**25**, 72%

entry	phenol A	phenol B	biphenol A-B
		$N_B \approx N_A$	
14		R = 4-Me	**7**, 40%
15		R = 4-t-Bu	**8**, 53%
16		R = 2-Me,6-OMe	**9**, 26%
17		R = 2,4-diOMe	**10**, 33%
18		R = 3,4-diMe	**26**, 47%
19			**27**, 46%
20		R = 2,4-diMe	**28**, 52%
21		R = 4-Me	**29**, 46%
22			**30**, 61%
23			**31a** (R^1= H, R^2= Me), 44% **31b** (R^1= Me, R^2= H), 39%

(1 equiv), which has a moderate N value (3.78 eV), was reacted under our general conditions with various phenols (1 equiv) that have a range of N values (as low as 3.08 eV for **1g** and up to 4.27 eV for **1l**). The cross-coupling products were isolated and plotted against ΔN (Figure 4). The results clearly show a good correlation between the ΔN values and the selectivity: for positive ΔN values, the cross-coupling was favored, while the coupling between two phenols with negative ΔN values was less selective and produced the cross-coupling products in low yields. This correlation further supports our premise that the difference in nucleophilicity of the two coupling partners plays a significant role in determining the reaction selectivity. Importantly, as mentioned above, the theoretical N index does not consider solvent effects; therefore, the true difference in nucleophilicity for a given pair of phenols can vary under different oxidation conditions.

Figure 5 displays a reactivity map (E_{ox} against N) in which the position of the phenol reflects its relative reactivity with regard to other phenols. On the basis of this reactivity map, we derived and tested our predictive model. For example, the coupling between phenolic component **1a** (1 equiv) and 3,4,5-trimethoxyphenol (**1l**, 3 equiv), which has positive ΔN value, was found to be highly selective, resulting in cross-coupling product **11** in 85% yield (Figure 5, insert 1 and red dashed line). At the other extreme, the coupling of phenol **1a** with the poorly nucleophilic 4-bromophenol (**1g**, $N_B \ll N_A$) failed to produce the required cross-coupling product **6**; rather, this resulted in an exclusively homocoupling product **2** (insert 2 and blue dashed line).

Both E_{ox} and N values are linked to structurally related properties. Therefore, in principle, as long as the oxidative coupling follows a radical−anion mechanism, these parameters can be used

to predict the feasibility of cross-coupling for a given pair of phenols. Indeed, when other oxidative cross-coupling methods were reviewed, a good agreement with our predictive model was observed. The Kozlowski group reported the aerobic oxidative cross-coupling of 3,5-dimethylphenol (**1m**, 1 equiv) with 2,6-di-*tert*-butylphenol (**1n**, 2 equiv) by a Cr(salen) complex. These two phenols have complementary E_{ox} and N values and produced coupling product **12** in 56% (91% brsm) yield (Scheme 4a and brown dashed line in Figure 5).[3b] The Katsuki group attempted the iron(salan)-catalyzed coupling of two naphthols with similar N values, 6-carbomethoxy-2-naphthol (**1o**, 2 equiv) and 3-bromo-2-naphthol (**1p**, 1 equiv), but the reaction proved to be challenging and was successful only if the concentration of naphthol **1p** was kept low throughout the reaction; unsymmetrical BINOL **13** was produced in 54% yield (93% ee, Scheme 4b and gray dashed line in Figure 5). In another example, the Waldvogel group applied an electrochemical oxidative coupling method to couple 2-methoxy-4-methylphenol (**1q**) with 2,4-dimethylphenol (**1d**). These phenols have a noncomplementary relationship ($\Delta N < 0$), and therefore, an excess of phenol **1d** (3 equiv) had to be used to produce unsymmetrical biphenol **14** in a satisfactory 52% yield (Scheme 4c and purple dashed line in Figure 5).[3c]

Reaction Scope. Finally, the applicability of the predictive model was examined for the coupling of different phenols and 2-naphthols under our iron-catalyzed oxidative coupling conditions. A mixture of FeCl$_3$ (10 mol %), phenol **A** (1 equiv), and phenol **B** (1−3 equiv) was stirred in HFIP (0.5 M) at room temperature for 30 min prior to the addition of *t*-BuOO*t*-Bu (1.5 equiv). The coupling between readily oxidized phenols with powerful nucleophilic 2-naphthol derivatives or 3,4,5-trimethoxyphenol (**1l**) took place in a selective manner, affording the desired unsymmetrical biphenols **4**, **11**, and **15−25** in moderate to excellent yields (Table 3, entries 1−13). In these reactions, there is a complementary E_{ox}−N relationship (E_{ox}**A** < E_{ox}**B**, $\Delta N \gg 0$), and cross-coupling products were formed with high selectivity and moderate to excellent yields. The cross-coupling between phenols that have N values in the same range (E_{ox}**A** < E_{ox}**B**, $N_B \approx N_A$) were less selective, and an excess of phenol **B** had to be used to improve the yield of the cross-coupling product (biphenols **7−10** and **26−31**). For example, the coupling of **1a** with 4-*tert*-butylphenol (**1i**, 1 equiv), whose nucleophilic power is lower than that of its coupling partner, produced a mixture of homocoupling product **2** (30% yield) and unsymmetrical biphenol **8** in 36% yield. The yield of the cross-coupling product was improved to 53% by using an excess (3 equiv) of nucleophile **1i** (entry 15).

In a radical−anion coupling mechanism, the regioselectivity is determined by the structure and properties of the two phenol substrates. While the coupling for the phenoxyl **A•** radical is restricted to the *para-* and *ortho-*positions, nucleophilic phenol **B** reacts at the most nucleophilic aromatic carbons. In such cases, in which the nucleophile has two reactive sites, such as in 3,5-dimethoxyphenol (**1r**), a mixture of isomers will be obtained, that is, biphenols **31a** and **31b** (45 and 40% yield, respectively). When the most nucleophilic site is substituted with methoxy or methyl groups, an oxidative addition/dearomatization step may occur, such as for dienones **11**, **24**, and **25** and enone **23**.

CONCLUSIONS

In summary, an efficient oxidative cross-coupling of phenols, using an iron salt as the catalyst and HFIP as the solvent, was developed. Our kinetic studies support a chelated radical−anion coupling mechanism in which both phenolic components are attached to the catalyst during the carbon−carbon forming step. To predict the feasibility of cross-coupling for a given pair of phenols **A** and **B**, we enhanced the Kočovský premise[3k] and hypothesized that, under a radical−anion coupling mechanism, a cross-coupling reaction will take place if the oxidation of phenol **A** to a phenoxyl **A•** radical in the presence of a stronger nucleophile phenol **B** is selective (E_{ox}**A** < E_{ox}**B** and $N_B > N_A$). The oxidation potentials (E_{ox}) and the theoretical global nucleophilicity (N) parameters of about 40 phenols were determined, and *a predictive model was proposed and successfully validated*. Several phenol−naphthol and phenol−phenol coupling reactions were performed, producing highly desired unsymmetrical biphenols in a single synthetic step.

ASSOCIATED CONTENT

Ⓢ Supporting Information
The Supporting Information is available free of charge on the ACS Publications website at DOI: 10.1021/jacs.5b06494.

> Full experimental procedures, characterization data, and NMR spectra (PDF)
> Additional tables and figure (PDF)

AUTHOR INFORMATION

Corresponding Author
*pappod@bgu.ac.il

Author Contributions
†A.L. and H.S. contributed equally.

Notes
The authors declare no competing financial interest.

REFERENCES

(1) (a) Kočovský, P.; Vyskočil, Š.; Smrčina, M. *Chem. Rev.* **2003**, *103*, 3213−3246. (b) Wang, H. *Chirality* **2010**, *22*, 827−837. (c) Brunel, J. M. *Chem. Rev.* **2005**, *105*, 857−898.
(2) Kobayashi, S.; Higashimura, H. *Prog. Polym. Sci.* **2003**, *28*, 1015−1048.
(3) (a) More, N. Y.; Jeganmohan, M. *Org. Lett.* **2015**, *17*, 3042. (b) Lee, Y. E.; Cao, T.; Torruellas, C.; Kozlowski, M. C. *J. Am. Chem. Soc.* **2014**, *136*, 6782−6785. (c) Elsler, B.; Schollmeyer, D.; Dyballa, K. M.; Franke, R.; Waldvogel, S. R. *Angew. Chem., Int. Ed.* **2014**, *53*, 5210−5213. (d) Huang, C.; Gevorgyan, V. *Org. Lett.* **2010**, *12*, 2442−2445. (e) Egami, H.; Matsumoto, K.; Oguma, T.; Kunisu, T.; Katsuki, T. *J. Am. Chem. Soc.* **2010**, *132*, 13633−13635. (f) Egami, H.; Katsuki, T. *J. Am. Chem. Soc.* **2009**, *131*, 6082−6083. (g) Guo, Q.-X.; Wu, Z.-J.; Luo, Z.-B.; Liu, Q.-Z.; Ye, J.-L.; Luo, S.-W.; Cun, L.-F.; Gong, L.-Z. *J. Am. Chem. Soc.* **2007**, *129*, 13927−13938. (h) Temma, T.; Hatano, B.; Habaue, S. *Tetrahedron* **2006**, *62*, 8559−8563. (i) Temma, T.; Habaue, S. *Tetrahedron Lett.* **2005**, *46*, 5655−5657. (j) Vyskocil, S.; Smrcina, M.; Lorenc, M.; Kocovsky, P.; Vyskocil, S.; Lorenc, M.; Hanus, V.; Polasek, M. *Chem. Commun.* **1998**, 585−586. (k) Smrcina, M.; Vyskocil, S.; Maca, B.; Polasek, M.; Claxton, T. A.; Abbott, A. P.; Kocovsky, P. *J. Org. Chem.* **1994**, *59*, 2156−2163. (l) Smrcina, M.; Polakova, J.; Vyskocil, S.; Kocovsky, P. *J. Org. Chem.* **1993**, *58*, 4534−4538. (m) Smrcina, M.; Lorenc, M.; Hanus, V.; Sedmera, P.; Kocovsky, P. *J. Org. Chem.* **1992**, *57*, 1917−1920. (n) Hovorka, M.; Ščigel, R.; Gunterová, J.; Tichý, M.; Závada, J. *Tetrahedron* **1992**, *48*, 9503−9516. (o) Hovorka, M.; Zavada, J. *Tetrahedron* **1992**, *48*, 9517−9530. (p) Hovorka, M.; Gunterova, J.; Zavada, J. *Tetrahedron Lett.* **1990**, *31*, 413−416. (q) Holtz-Mulholland, M.; de Leseleuc, M.; Collins, S. K. *Chem. Commun* **2013**, *49*, 1835−1837.

(4) (a) Gaster, E.; Vainer, Y.; Regev, A.; Narute, S.; Sudheendran, K.; Werbeloff, A.; Shalit, H.; Pappo, D. *Angew. Chem., Int. Ed.* **2015**, *54*, 4198−4202. (b) Regev, A.; Shalit, H.; Pappo, D. *Synthesis* **2015**, *47*, 1716−1725. (c) Kshirsagar, U. A.; Regev, C.; Parnes, R.; Pappo, D. *Org. Lett.* **2013**, *15*, 3174−3177. (d) Kshirsagar, U. A.; Parnes, R.; Goldshtein, H.; Ofir, R.; Zarivach, R.; Pappo, D. *Chem. - Eur. J.* **2013**, *19*, 13575−13583. (e) Parnes, R.; Kshirsagar, U. A.; Werbeloff, A.; Regev, C.; Pappo, D. *Org. Lett.* **2012**, *14*, 3324−3327.

(5) (a) Li, C. J. *Acc. Chem. Res.* **2009**, *42*, 335−344. (b) Scheuermann, C. J. *Chem. - Asian J.* **2010**, *5*, 436−451. (c) Girard, S. A.; Knauber, T.; Li, C. J. *Angew. Chem., Int. Ed.* **2014**, *53*, 74−100. (d) Li, Z.; Li, C.-J. *J. Am. Chem. Soc.* **2005**, *127*, 3672−3673. (e) Li, Z.; Li, C.-J. *J. Am. Chem. Soc.* **2004**, *126*, 11810−11811. (f) Yeung, C. S.; Dong, V. M. *Chem. Rev.* **2011**, *111*, 1215−1292. (g) Li, Z.; Bohle, D. S.; Li, C.-J. *Proc. Natl. Acad. Sci. U. S. A.* **2006**, *103*, 8928−8933. (h) Jia, F.; Li, Z. *Org. Chem. Front.* **2014**, *1*, 194−214. (i) Studer, A.; Curran, D. P. *Nat. Chem.* **2014**, *6*, 765−773. (j) Liu, C.; Liu, D.; Lei, A. *Acc. Chem. Res.* **2014**, *47*, 3459−3470.

(6) (a) Enthaler, S.; Junge, K.; Beller, M. *Angew. Chem., Int. Ed.* **2008**, *47*, 3317−3321. (b) Bolm, C.; Legros, J.; Le Paih, J.; Zani, L. *Chem. Rev.* **2004**, *104*, 6217−6254. (c) Bauer, I.; Knölker, H.-J. *Chem. Rev.* **2015**, *115*, 3170−3387. (d) Guo, X.; Yu, R.; Li, H.; Li, Z. *J. Am. Chem. Soc.* **2009**, *131*, 17387−17393.

(7) (a) Vuluga, D.; Legros, J.; Crousse, B.; Slawin, A. M. Z.; Laurence, C.; Nicolet, P.; Bonnet-Delpon, D. l. *J. Org. Chem.* **2011**, *76*, 1126−1133. (b) Shuklov, I. A.; Dubrovina, N. V.; Börner, A. *Synthesis* **2007**, *2007*, 2925−2943. (c) Berkessel, A.; Adrio, J. A.; Hüttenhain, D.; Neudörfl, J. M. *J. Am. Chem. Soc.* **2006**, *128*, 8421−8426. (d) Berkessel, A.; Adrio, J. A. *J. Am. Chem. Soc.* **2006**, *128*, 13412−13420. (e) Bégué, J.-P.; Bonnet-Delpon, D.; Crousse, B. *Synlett* **2004**, *2004*, 18−29. (f) de Visser, S. P.; Kaneti, J.; Neumann, R.; Shaik, S. *J. Org. Chem.* **2003**, *68*, 2903−2912.

(8) (a) Dohi, T.; Yamaoka, N.; Kita, Y. *Tetrahedron* **2010**, *66*, 5775−5785. (b) Hamamoto, H.; Anilkumar, G.; Tohma, H.; Kita, Y. *Chem. - Eur. J.* **2002**, *8*, 5377−5383. (c) Eberson, L.; Hartshorn, M. P.; Persson, O.; Radner, F. *Chem. Commun.* **1996**, 2105−2112. (d) Lucarini, M.; Pedulli, G. F.; Guerra, M. *Chem. - Eur. J.* **2004**, *10*, 933−939.

(9) (a) Foti, M. C.; Amorati, R.; Pedulli, G. F.; Daquino, C.; Pratt, D. A.; Ingold, K. U. *J. Org. Chem.* **2010**, *75*, 4434−4440. (b) de Heer, M. I.; Korth, H.-G.; Mulder, P. *J. Org. Chem.* **1999**, *64*, 6969−6975.

(10) Lucarini, M.; Mugnaini, V.; Pedulli, G. F.; Guerra, M. *J. Am. Chem. Soc.* **2003**, *125*, 8318−8329.

(11) (a) Boldron, C.; Aromi, G.; Challa, G.; Gamez, P.; Reedijk, J. *Chem. Commun.* **2005**, 5808−5810. (b) Ogata, M.; Shin-ya, K.; Urano, S.; Endo, T. *Chem. Pharm. Bull.* **2005**, *53*, 344−346. (c) Kirste, A.; Schnakenburg, G.; Waldvogel, S. R. *Org. Lett.* **2011**, *13*, 3126−3129. (d) Purohit, C. S.; Parvez, M.; Verma, S. *Appl. Catal., A* **2007**, *316*, 100−106.

(12) (a) Ingold, K. U.; Pratt, D. A. *Chem. Rev.* **2014**, *114*, 9022−9046. (b) Wu, Y.-D.; Lai, D. K. W. *J. Org. Chem.* **1996**, *61*, 7904−7910. (c) Estácio, S. G.; Cabral do Couto, P.; Costa Cabral, B. J.; Minas da Piedade, M. E.; Martinho Simões, J. A. *J. Phys. Chem. A* **2004**, *108*, 10834−10843. (d) Borges dos Santos, R. M.; Martinho Simões, J. A. *J. Phys. Chem. Ref. Data* **1998**, *27*, 707−739. (e) Klein, E.; Lukeš, V. *Chem. Phys.* **2006**, *330*, 515−525.

(13) Wright, J. S.; Johnson, E. R.; DiLabio, G. A. *J. Am. Chem. Soc.* **2001**, *123*, 1173−1183.

(14) (a) Domingo, L. R.; Chamorro, E.; Pérez, P. *J. Org. Chem.* **2008**, *73*, 4615−4624. (b) Domingo, L. R.; Perez, P. *Org. Biomol. Chem.* **2011**, *9*, 7168−7175.

(15) Pratihar, S.; Roy, S. *J. Org. Chem.* **2010**, *75*, 4957−4963.

(16) Mayr, H.; Kempf, B.; Ofial, A. R. *Acc. Chem. Res.* **2003**, *36*, 66−77.

(17) Boess, E.; Schmitz, C.; Klussmann, M. *J. Am. Chem. Soc.* **2012**, *134*, 5317−5325.